

Supporting Information

Hydrogen bonds regulation to enhance catalytic C-C bonds cleavage of polylactic acid wastes in H₂O to produce H₂

This file includes:

Supplementary Methods

Supplementary Figure 1 to 10

Supplementary Table 1 to 10

References

Supplementary Methods

Chemicals and materials

Poly(lactic acid) (PLA) plastic particles, lactic acid, 3-hydroxypropanoic acid, glyceric acid and propanoic acid were purchased from Aladdin Chemistry CO., Ltd. PLA powder, fork, spoon, straw and cup were obtained from Liaoning Jinliang Biotechnology Co., Ltd. NaOH was acquired from Tianjin Kemiou Chemical Reagent Co., Ltd. DMSO- d_6 was purchased from Sigma-Aldrich. The different nickel-based catalyst precursors powders were obtained from Dalian Tongyong Chemical Co., Ltd. Carbon dioxide (>99%), methane (>99%), ethane (>99%), propane (>99%), butane (>99%), hydrogen (>99%) and the mixed standard gas were obtained from Zhengzhou Gas Products Co., Ltd. Milli-Q water was used in all experiments.

Characterization

Scanning electron microscopy (SEM) characterization: SEM was conducted on a JEM-7800F (JEOL) microscope, and it was operated at 1.0 kV.

Transmission electron microscopy (TEM) characterization: TEM and EDS elemental maps were performed with JEM-2100 (JEOL) microscope, the operated voltage was 200 kV.

Inductively coupled plasma-optical emission spectrometry (ICP-OES) analysis: ICP-OES was conducted by ICPS-8100 (Shimadzu), which was operated with the radio-frequency power of 1.0 kW. The catalyst was dissolved in aqua regia and then diluted to a certain volume in the volumetric flask.

X-ray diffraction (XRD) analysis: XRD was carried out with the Rigaku D/Max 2500/PC

diffractometer, Cu K α radiation ($\lambda = 0.15418$ nm) was operated at 40 kV/200 mA. And the wide-angle patterns were scanned from 10° to 90° (2θ) at a scan rate of 2.5° min⁻¹.

¹H nuclear magnetic resonance (NMR) spectra: NMR analysis was conducted on a Bruker ADVANCE III 400 MHz spectrometer. Lactic acid, lactic acid and H₂O mixture were operated from 25 to 50 °C in DMSO-*d*₆.

Density functional theory (DFT) calculations: The first-principles^{1,2} was employed to perform DFT calculations within the generalized gradient approximation (GGA) using the Perdew-Burke-Ernzerhof (PBE) formulation.³ We have chosen the projected augmented wave (PAW) potentials^{4,5} to describe the ionic cores and take valence electrons into account using a plane wave basis set with a kinetic energy cutoff of 520 eV. Partial occupancies of the Kohn-Sham orbitals were allowed using the Gaussian smearing method with a width of 0.05 eV. The electronic energy was considered self-consistent when the energy change was smaller than 10⁻⁶ eV. A geometry optimization was considered convergent when the energy change was smaller than 0.03 eV Å⁻¹. In this structure, the U correction was used for Ni (4.96 eV) and Fe (4.66 eV) atoms. The vacuum spacing in a direction perpendicular to the plane of the structure is 20 Å for the surfaces. The Brillouin zone integration is performed using 2×2×1 Monkhorst-Pack k-point sampling for a structure. The free energy was calculated using the equation:

$$G = E_{\text{ads}} + \text{ZPE} - \text{TS} \quad (1)$$

where G , E_{ads} , ZPE and TS were the free energy, total energy from DFT calculations, zero-point energy and entropic contributions, respectively. Finally, transition states for elementary reaction steps were determined by a combination of the nudged elastic band (NEB) method⁶

and the dimer method.⁷⁻⁹ In the NEB method, the path between the reactant and product was discretized into a series of structural images. The image that was closest to a likely transition state structure, which was then employed as an initial guess structure for the dimer method.

Supplementary Figure

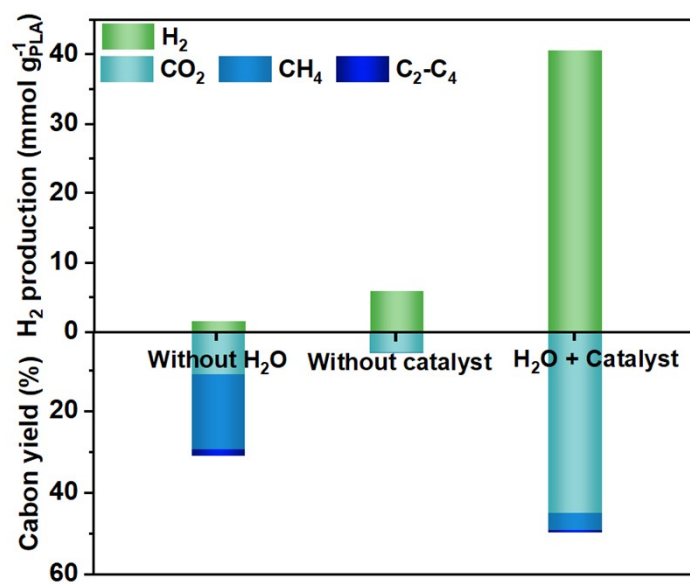


Fig. S1 Influence of catalyst and H₂O on the conversion of PLA to H₂. Reaction condition:

0.2 g PLA, 1.5 mmol Ni-Fe catalyst, 15 mL H₂O, 10 bar N₂, 300 °C, 5 h.

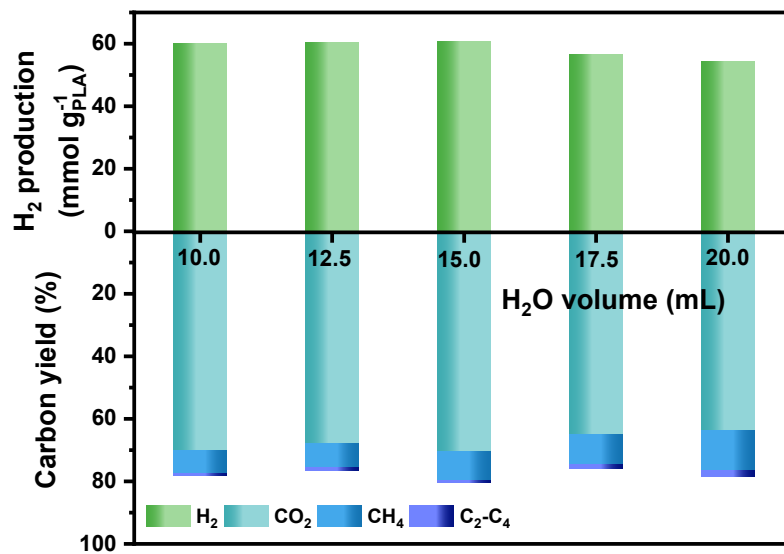


Fig. S2 Effect of H₂O volume on the catalytic conversion of PLA to H₂. Reaction condition:

0.2 g PLA, 1.5 mmol Ni-Fe catalyst, H₂O, 10 bar N₂, 310 °C, 5 h.

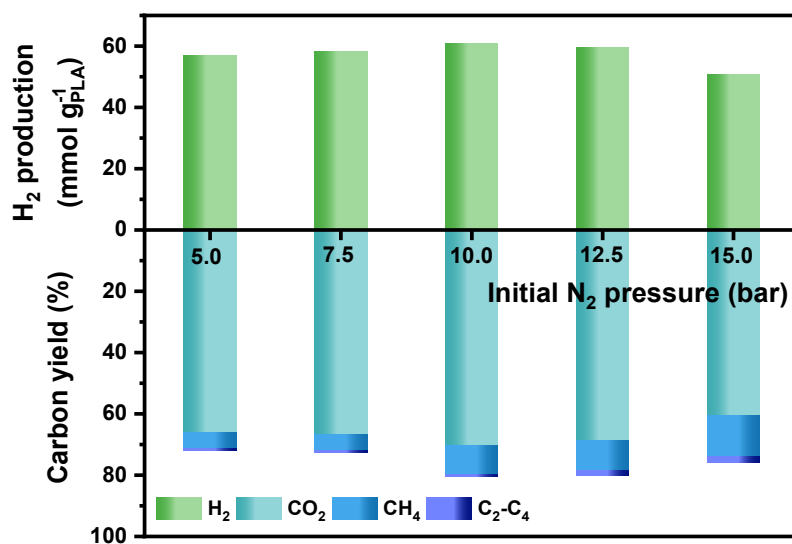


Fig. S3 Effect of initial N₂ pressure on the catalytic conversion of PLA to H₂. Reaction condition: 0.2 g PLA, 1.5 mmol Ni-Fe catalyst, 15 mL H₂O, 310 °C, 5 h.

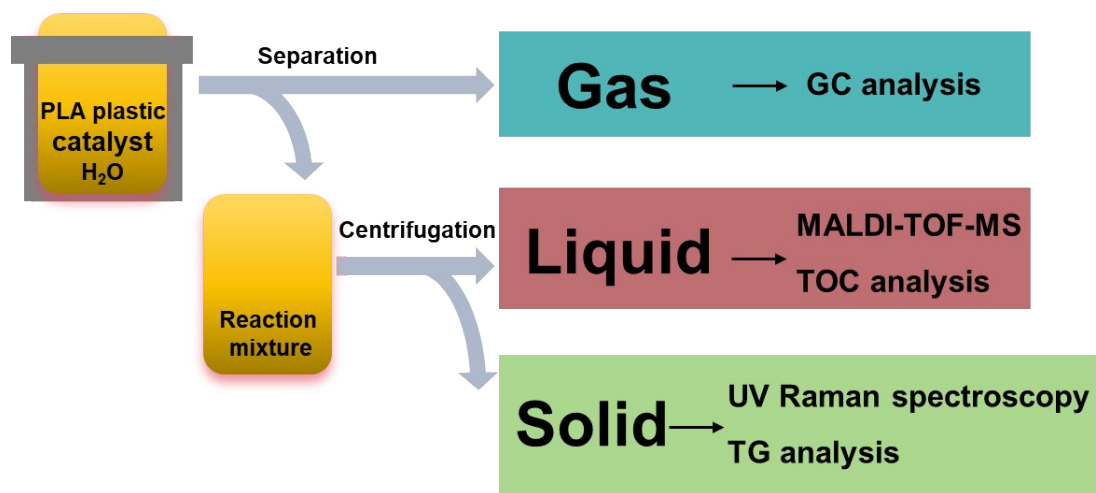


Fig. S4 The products analysis for the catalytic transformation of PLA. The gas, liquid and solid products were collected and analyzed after reaction.

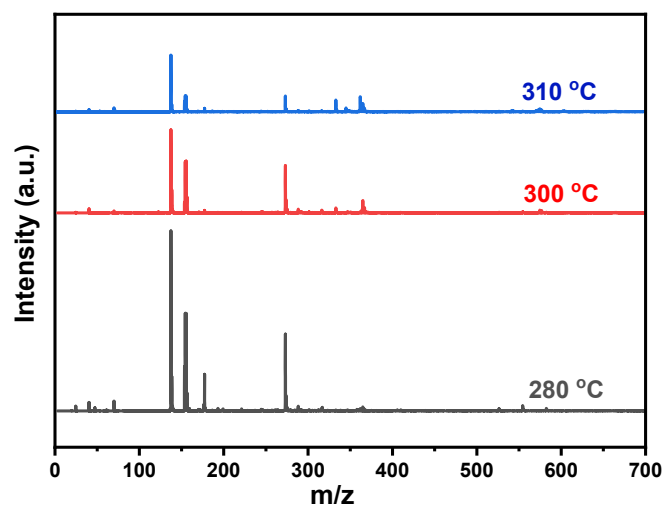


Fig. S5 MALDI-TOF-MS spectra of liquid products with different reaction temperatures.

Reaction condition: 0.2 g PLA, 1.5 mmol Ni-Fe catalyst, 15 mL H₂O, 10 bar N₂, 5 h.

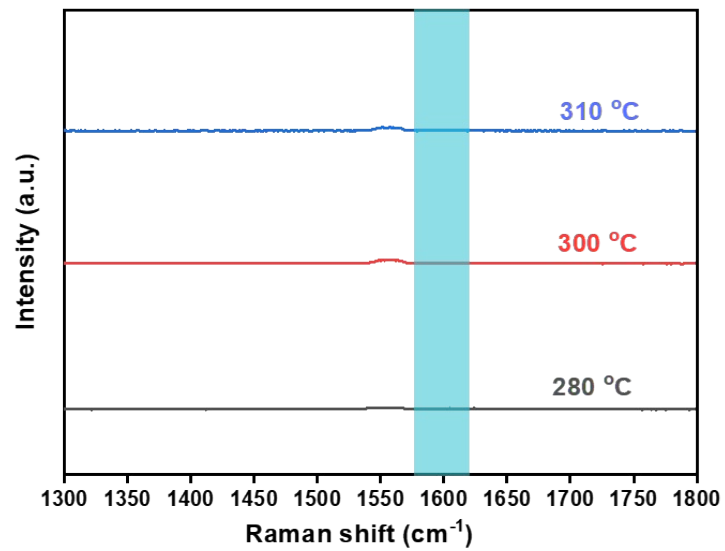


Fig. S6 UV Raman spectra of solid residue with different reaction temperatures. Reaction condition: 0.2 g PLA, 1.5 mmol Ni-Fe catalyst, 15 mL H₂O, 10 bar N₂, 5 h.

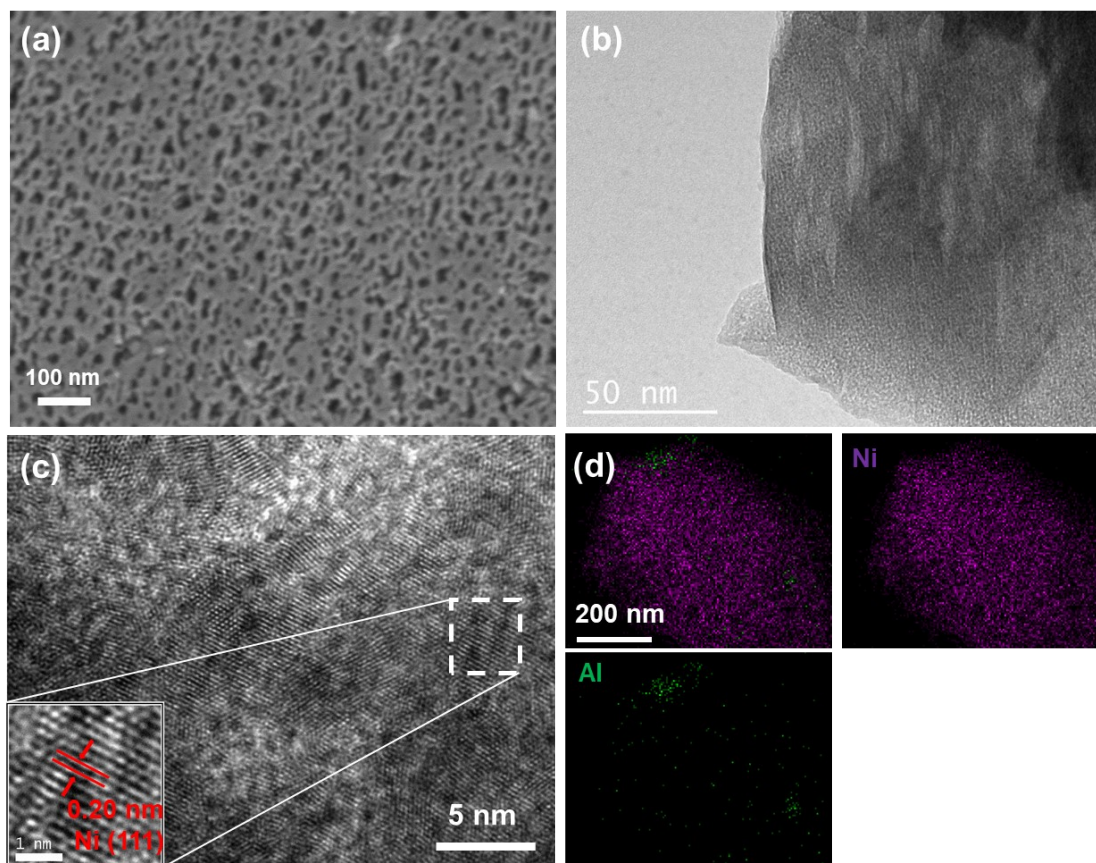


Fig. S7 SEM and TEM images of Ni catalyst. (a) SEM image of Ni catalyst. (b-d) TEM images with EDS elemental mapping of Ni catalyst.

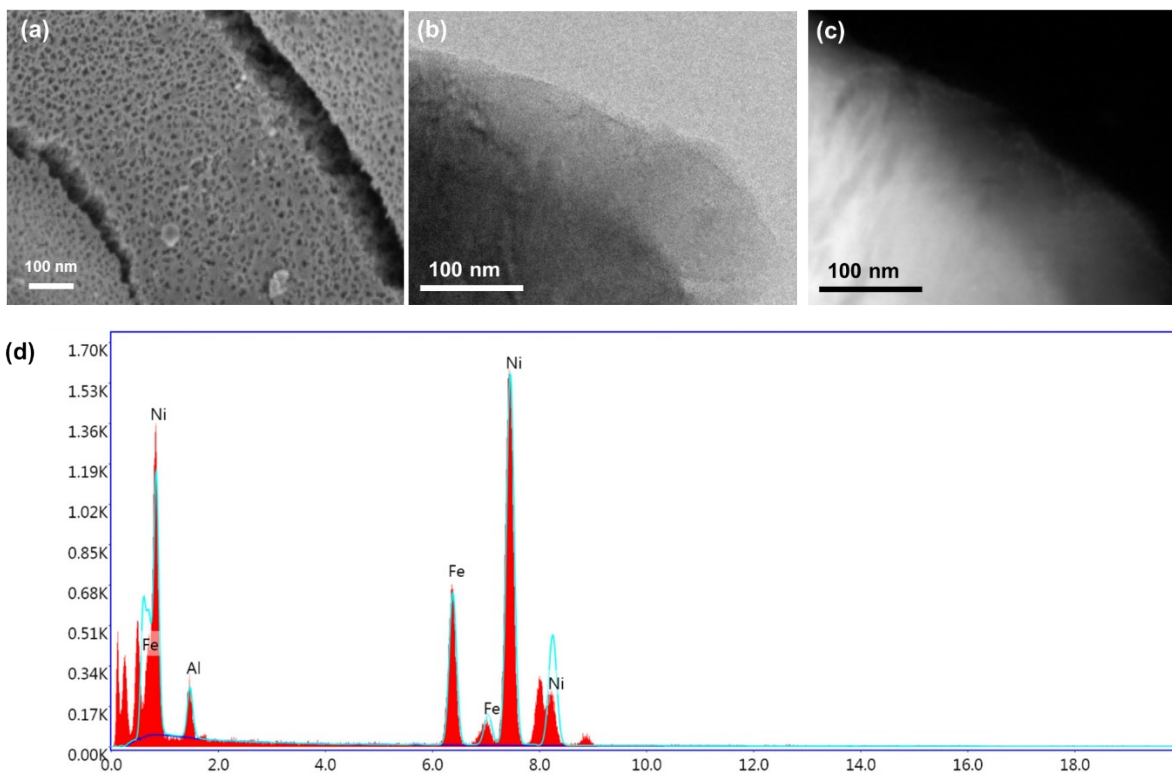


Fig. S8 SEM and TEM images of Ni-Fe catalyst. (a) SEM image of Ni-Fe catalyst. (b-d) STEM images with elemental analysis of Ni-Fe catalyst.

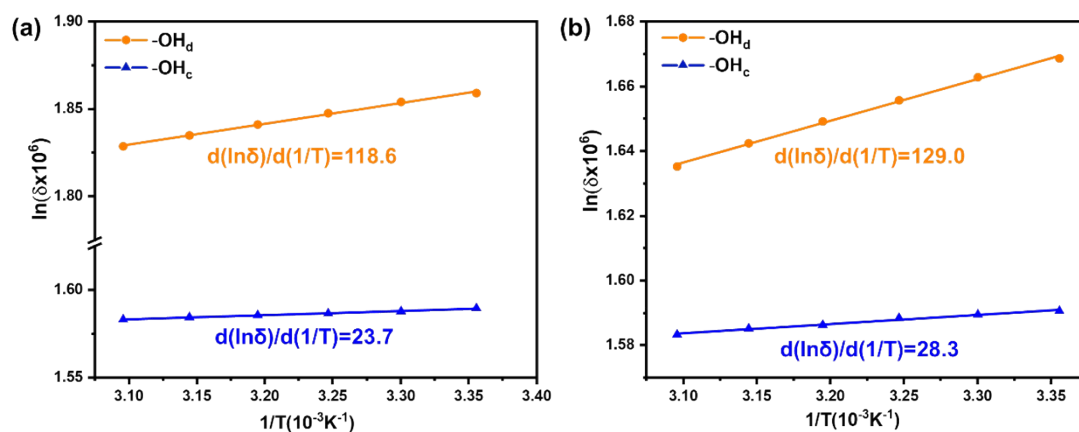


Fig. S9 Linear fits of $\ln\delta$ versus $1/T$. (a) Linear fits of $\ln\delta$ versus $1/T$ for $-\text{OH}_d$ and $-\text{OH}_c$ in lactic acid. (b) Linear fits of $\ln\delta$ versus $1/T$ for $-\text{OH}_d$ and $-\text{OH}_c$ in lactic acid and H_2O with the mole ratio of 1:1.

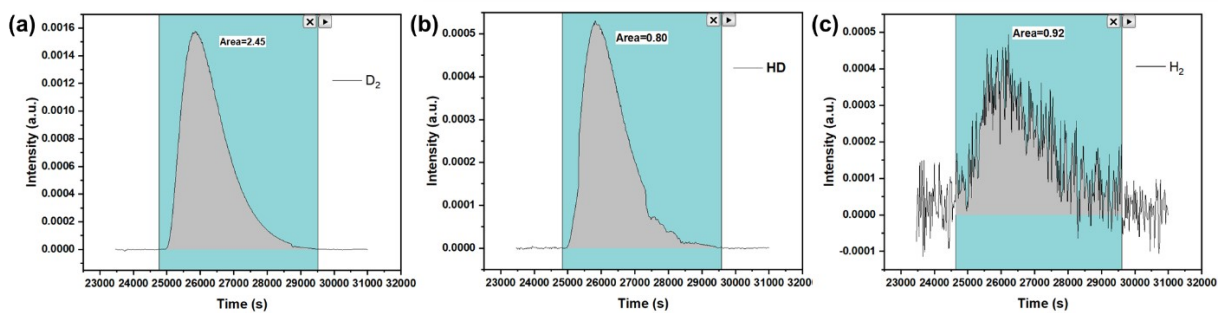


Fig. S10 Mass spectrometry analysis of hydrogen production from the catalytic conversion of PLA in qualitative and semi-quantitative. Reaction condition: 0.2 g PLA-based cup, 1.5 mmol Ni-Fe catalyst, 15 mL D_2O , 10 bar N_2 , 310 °C, 5 h.

Supplementary Table

Table S1 H₂ production, H₂ selectivity, carbon yield of gas products and the detailed distribution of CO₂, CH₄ and C₂-C₄ hydrocarbons over the different catalysts.

Entry ^a	Catalyst	H ₂ production (mmol g ⁻¹ PLA)	H ₂ selectivity (%)	Gas carbon yield (%)	Gas carbon products distribution (mol%)		
					CO ₂	CH ₄	C ₂ -C ₄
1 ^b	Fe	10.3 _{±0}	63.0 _{±2.3}	19.8 _{±0.8}	77.0 _{±0.8}	20.2 _{±0.7}	2.8 _{±0}
2 ^c	Ni	22.4 _{±0.4}	79.2 _{±2.0}	34.0 _{±0.2}	85.8 _{±0.8}	13.0 _{±0.8}	1.2 _{±0}
3	Ni-Fe	40.6 _{±0.4}	98.4 _{±0.4}	49.7 _{±0.2}	90.5 _{±2.3}	8.4 _{±2.2}	1.1 _{±0.1}
4 ^d	Ni-Sn	20.9 _{±0.3}	57.7 _{±0.8}	43.0 _{±0.2}	74.1 _{±0.5}	21.8 _{±0.4}	4.2 _{±0.1}
5 ^e	Ni-Mo	19.0 _{±0.3}	89.2 _{±0}	25.5 _{±0.5}	91.6 _{±1.2}	7.5 _{±1.0}	0.9 _{±0}

^aThe hydrogen and carbon yield of gas products were quantified by GC analysis, reaction condition: 0.2 g PLA, 1.5 mmol Ni-Fe catalyst, 15 mL H₂O, 10 bar N₂, 300 °C, 5 h.

^b2.0 mmol Fe catalyst.

^c2.0 mmol Ni catalyst.

^d1.6 mmol Ni-Sn catalyst.

^e1.9 mmol Ni-Mo catalyst.

Table S2 H₂ production, H₂ selectivity, carbon yield of gas products and the detailed distribution of CO₂, CH₄ and C₂-C₄ hydrocarbons without H₂O or catalyst.

Entry ^a	Reaction condition	H ₂ production (mmol g _{PLA} ⁻¹)	Gas carbon yield (%)	Gas carbon products distribution (mol%)		
				CO ₂	CH ₄	C ₂ -C ₄
1	Without H ₂ O	1.5	30.9	35.7	59.3	5.0
2	Without catalyst	5.9	5.8	95.3	3.2	1.5
3	H ₂ O + Catalyst	40.6	49.7	90.5	8.4	1.1

^aReaction condition: 0.2 g PLA, 1.5 mmol Ni-Fe catalyst, 15 mL H₂O, 10 bar N₂, 300 °C, 5 h.

Table S3 H₂ production, H₂ selectivity, carbon yield of gas products and the detailed distribution of CO₂, CH₄ and C₂-C₄ hydrocarbons with the different reaction temperature.

Entry ^a	Reaction temperature (°C)	H ₂ production (mmol g _{PLA} ⁻¹)	Gas carbon yield (%)	Gas carbon products distribution (mol%)		
				CO ₂	CH ₄	C ₂ -C ₄
1	280	16.3 _{±0.4}	21.2 _{±0.1}	80.7 _{±1.3}	17.1 _{±1.4}	2.2 _{±0}
2	290	26.0 _{±0.3}	31.2 _{±0.3}	87.9 _{±0.2}	10.2 _{±0.1}	1.9 _{±0.1}
3	300	40.6 _{±0.4}	49.7 _{±0.2}	90.5 _{±2.3}	8.4 _{±2.2}	1.1 _{±0.1}
4	310	60.8 _{±0.2}	80.4 _{±0.5}	87.0 _{±0.1}	11.8 _{±0.2}	1.2 _{±0}
5	320	62.0 _{±0.3}	82.1 _{±0.2}	87.1 _{±0.5}	11.4 _{±0.4}	1.5 _{±0.1}

^aReaction condition: 0.2 g PLA, 1.5 mmol Ni-Fe catalyst, 15 mL H₂O, 10 bar N₂, 5 h.

Table S4 H₂ production, H₂ selectivity, carbon yield of gas products and the detailed distribution of CO₂, CH₄ and C₂-C₄ hydrocarbons with the different H₂O volume.

Entry ^a	H ₂ O volume (mL)	H ₂ production (mmol g _{PLA} ⁻¹)	H ₂ selectivity (%)	Gas carbon yield (%)	Gas carbon products distribution (mol%)		
					CO ₂	CH ₄	C ₂ -C ₄
1	10.0	60.2	92.4	78.2	89.6	9.3	1.1
2	12.5	60.3	94.7	76.4	89.0	9.8	1.2
3	15.0	60.8	90.7	80.4	87.0	11.8	1.2
4	17.5	56.6	89.3	76.0	85.7	12.6	1.7
5	20.0	54.2	83.1	78.4	81.2	16.4	2.4

^aReaction condition: 0.2 g PLA, 1.5 mmol Ni-Fe catalyst, H₂O, 10 bar N₂, 310 °C, 5 h.

Table S5 H₂ production, H₂ selectivity, carbon yield of gas products and the detailed distribution of CO₂, CH₄ and C₂-C₄ hydrocarbons with the different initial N₂ pressure.

Entry ^a	Initial N ₂ pressure (bar)	H ₂ production (mmol g _{PLA} ⁻¹)	H ₂ selectivity (%)	Gas carbon yield (%)	Gas carbon products distribution (mol%)		
					CO ₂	CH ₄	C ₂ -C ₄
1	5.0	57.0	95.1	72.0	91.6	7.3	1.1
2	7.5	58.3	96.4	72.6	91.7	7.2	1.1
3	10.0	60.8	90.7	80.4	87.0	11.8	1.2
4	12.5	59.6	89.2	80.1	85.7	12.3	2.0
5	15.0	50.7	80.2	76.0	79.8	17.5	2.7

^aReaction condition: 0.2 g PLA, 1.5 mmol Ni-Fe catalyst, 15 mL H₂O, N₂, 310 °C, 5 h.

Table S6 H₂ production, carbon yield of gas products and the detailed distribution of CO₂, CH₄ and C₂-C₄ hydrocarbons with the different reaction time.

Entry ^a	Reaction time (min)	H ₂ production (mmol g ⁻¹ PLA)	Gas carbon yield (%)	Gas carbon products distribution (mol%)		
				CO ₂	CH ₄	C ₂ -C ₄
1	10	16.7	21.5	91.3	8.0	0.7
2	30	23.6	29.5	86.5	12.6	0.9
3	60	32.4	37.8	90.0	9.3	0.7
4	120	54.5	70.9	87.3	11.3	1.4
5	180	56.9	72.2	87.7	10.9	1.4
6	300	60.8	80.4	87.0	11.8	1.2
7	420	60.8	78.7	86.6	11.8	1.6

^aReaction condition: 0.2 g PLA, 1.5 mmol Ni-Fe catalyst, 15 mL H₂O, 10 bar N₂, 310 °C.

Table S7 H₂ yield, carbon yield of gas products and the detailed distribution of CO₂, CH₄ and C₂-C₄ hydrocarbons from the model compounds conversion over Ni catalyst.

Entry ^a	Substrate	H ₂ yield (%)	Gas carbon yield (%)	Gas carbon products distribution (mol%)		
				CO ₂	CH ₄	C ₂ -C ₄
1	PLA	18.7	24.9	88.0	10.4	1.6
2	Lactic acid	20.8	21.6	87.6	10.6	1.8
3	Glyceric acid	47.5	62.1	86.4	13.1	0.5
4	Propionic acid	9.1	4.5	86.7	6.7	6.6
5	3-Hydroxypropionic acid	32.1	50.9	67.2	27.5	5.3

^aReaction condition: 0.2 g substrate, 2.0 mmol Ni catalyst, 15 mL H₂O, 10 bar N₂, 290 °C, 5 h.

Table S8 H₂ yield, carbon yield of gas products and the detailed distribution of CO₂, CH₄ and C₂-C₄ hydrocarbons from the model compounds conversion over Ni-Fe catalyst.

Entry ^a	Substrate	H ₂ yield (%)	Gas carbon yield (%)	Gas carbon products distribution (mol%)		
				CO ₂	CH ₄	C ₂ -C ₄
1	PLA	31.2	31.2	87.9	10.2	1.9
2	Lactic acid	39.7	41.6	92.7	6.1	1.2
3	Glyceric acid	70.8	82.0	82.5	16.2	1.3
4	Propionic acid	55.1	59.5	82.7	11.0	6.3
5	3-Hydroxypropionic acid	71.7	81.2	80.9	14.4	4.7

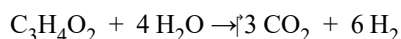
^aReaction condition: 0.2 g substrate, 1.5 mmol Ni-Fe catalyst, 15 mL H₂O, 10 bar N₂, 290 °C, 5 h.

Table S9 The content of C, H and O in PLA plastic wastes.

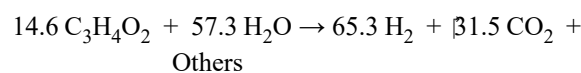
Entry ^a	Substrate	C (%)	H (%)	O (%)	Others (%)
1	Powder	50.3	5.4	43.6	0.7
2	Fork-spoon	37.5	4.2	32.6	25.7
3	Straw	42.7	4.4	35.7	17.2
4	Cup	49.9	5.3	43.2	1.6

^aAccording to the content of C, H and O in PLA plastic wastes, the mole numbers of C, H and O in a certain amount of PLA plastic wastes could be calculated. Others contained N, S and ash.

In our work, the content of C, H and O in PLA-based cup was measured, which could be denoted as a chemical formula of C₃H₄O₂. For the catalytic conversion of PLA-based cup to CO₂ and H₂, the theoretical chemical equation was shown as follows:



However, in our experiment, some other gas products, such as CH₄ and C₂-C₄ hydrocarbons, also generated. And the coefficient of gas products was determined on the basis of the mole percentage of gas products after the reaction at 310 °C. Furthermore, the coefficient of C₃H₄O₂ and H₂O was calculated according to the gas carbon yield and hydrogen yield. Ultimately, the chemical equation based on our experiment results was shown below:



Hereinto, others included the deposited carbon species and small amount of organic molecules, etc.

Table S10 H₂ production, H₂ selectivity, carbon yield of gas products and the detailed distribution of CO₂, CH₄ and C₂-C₄ hydrocarbons with different PC plastic wastes.

Entry ^a	Substrate	H ₂ production (mmol g ⁻¹ _{plastic})	H ₂ selectivity (%)	Gas carbon yield (%)	Gas carbon products distribution (mol%)		
					CO ₂	CH ₄	C ₂ -C ₄
1	Powder	53.8 _{±0.5}	97.4 _{±0.2}	66.3 _{±0.7}	90.1 _{±0.3}	8.8 _{±0.3}	1.1 _{±0}
2	Fork-spoon	49.3 _{±0.3}	98.9 _{±0.7}	59.8 _{±0.7}	91.0 _{±0.4}	7.7 _{±0.4}	1.3 _{±0}
3	Straw	52.0 _{±0.1}	99.8 _{±0}	62.6 _{±0.1}	90.9 _{±0.5}	8.0 _{±0.4}	1.1 _{±0}
4	Cup	62.6 _{±0.2}	93.5 _{±0.2}	80.5 _{±0.1}	90.1 _{±0.2}	8.6 _{±0.2}	1.3 _{±0}

^aReaction condition: 0.2 g PLA-based substrates, 1.5 mmol Ni-Fe catalyst, 15 mL H₂O, 10 bar N₂, 310 °C, 5 h.

Reference

- [1] G. Kresse and J. Furthmüller, *Comp. Mater. Sci.*, 1996, **6**, 15-50.
- [2] G. Kresse and J. Furthmüller, *Phys. Rev. B*, 1996, **54**, 11169-11186.
- [3] J. P. Perdew, K. Burke and M. Ernzerhof, *Phys. Rev. Lett.*, 1996, **77**, 3865-3868.
- [4] G. Kresse and D. Joubert, *Phys. Rev. B*, 1999, **59**, 1758-1775.
- [5] P. E. Blöchl, *Phys. Rev. B*, 1994, **50**, 17953-17979.
- [6] G. Henkelman, B. P. Uberuaga and H. Jonsson, *J. Chem. Phys.*, 2000, **113**, 9901.
- [7] G. Henkelman and H. Jonsson, *J. Chem. Phys.*, 1999, **111**, 7010-7022.
- [8] R. A. Olsen, G. J. Kroes, G. Henkelman, A. Arnaldsson and H. Jónsson, *J. Chem. Phys.*, 2004, **121**, 9776-9792.
- [9] A. Heyden, A. T. Bell and F. J. Keil, *J. Chem. Phys.*, 2005, **123**, 224101.